Athens Institute for Education and Research
ATINER

ATINER's Conference Paper Series
CIV2016-2128

Optimization of a Vertical Axis Wind Turbine Using FEA, Multibody Dynamics and Wind Tunnel Testing

Jihad Rishmany
Assistant Professor
University of Balamand
Lebanon

Michel Daaboul
Associate Professor
University of Balamand
Lebanon

Issam Tawk
Assistant Professor
University of Balamand
Lebanon

Nicolas Saba
Assistant Professor
University of Balamand
Lebanon

ATINER CONFERENCE PAPER SERIES No: CIV2016-2128

An Introduction to ATINER's Conference Paper Series

ATINER started to publish this conference papers series in 2012. It includes only the papers submitted for publication after they were presented at one of the conferences organized by our Institute every year. This paper has been peer reviewed by at least two academic members of ATINER.

Dr. Gregory T. Papanikos
President
Athens Institute for Education and Research

This paper should be cited as follows:

Rishmany, J., Daaboul, M., Tawk, I. and Saba, N. (2016). **"Optimization of a Vertical Axis Wind Turbine Using FEA, Multibody Dynamics and Wind Tunnel Testing",** Athens: ATINER'S Conference Paper Series, No: **CIV2016-2128.**

Athens Institute for Education and Research
8 Valaoritou Street, Kolonaki, 10671 Athens, Greece
Tel: + 30 210 3634210 Fax: + 30 210 3634209 Email: info@atiner.gr URL: www.atiner.gr
URL Conference Papers Series: www.atiner.gr/papers.htm

ISSN: 2241-2891
13/02/2017

Optimization of a Vertical Axis Wind Turbine Using FEA, Multibody Dynamics and Wind Tunnel Testing

Jihad Rishmany
Michel Daaboul
Issam Tawk
Nicolas Saba

Abstract

Wind as a renewable energy source is not yet fully exploited despite the permanent availability of this source. Moreover, in countries where renewable energy regulations are still absent, big scale application is still non-applicable. In this context, a domestic vertical axis wind turbine is designed and tested. Design phases first included a series of wind tunnel tests in order to select the appropriate airfoil geometry and the optimum number of blades. Scaling was then applied in order to obtain a desired output power. Optimization of system performance and appropriate component selection were realized with the aid of a multi-body dynamics analysis tool and finite element analysis.

Keywords: FEA, Multibody dynamics, Optimization, VAWT, Wind Tunnel Testing.

Introduction

Wind energy is not an invention of our time. Around 5000 B.C, ancient Egyptians found out that they can rely on the wind to enhance their navigation through the Nile River (Kaldellis and Zafirakis, 2011). Later on, the invention of windmills helped Persian in grains grinding and water pumping (Yannopoulos et al., 2015). The breakthrough of wind energy took place in the 19^{th} century by the generation of electricity (Righter, 1996). Starting in the 1920s, wind turbines were used on larger scale, and were installed over a numerous number of farms to power lights and many electrical appliances such as washing machines and radios (Wilson, 1969).

Several studies were conducted on the investigation of wind turbines for energy generation, through experiments (Darrieus, 1931; Lee et al., 2016, Li et al., 2016) and numerical simulations (Roy and Saha, 2013; Roy and Ducoin, 2016; Balduzzi et al., 2016). Assessment on performance has been widely carried out in several works (Tjiu et al., 2015).

Types of Wind Turbines

In general, there are two major types of wind turbines: horizontal axis wind turbine (HAWT) and vertical axis wind turbine (VAWT). The HAWT turbine is mounted on a large tower and has in general two or three blades and its axis is parallel to the wind flow. The difference in wind speeds on the top and bottom side creates a difference in pressure between the blade surfaces so that an aerodynamic lift is produced. Moreover, there exists a drag force perpendicular to the lift force which opposes the rotation of the turbine (Eriksson et al., 2008). Furthermore, there are mainly two types of HAWT turbines: upwind turbine and downwind turbine.

The VAWT turbine has its rotor positioned vertically. The advantages of VAWT turbines become clear when operating at a low speed. There are mainly two main types of VAWT: Savonius and Darrieus.

The Savonius wind turbine is well known to be a drag type turbine. This type of turbine has low efficiency in general but it is suitable for areas with turbulent wind. The Darrieus wind turbine needs a motor to start its motion. It is also well suited for places with turbulent wind where it shows high efficiency (Can et al., 2010).

Figure **1** presents 4 different types of wind turbines.

Figure 1. *Common Types of Wind Turbines*

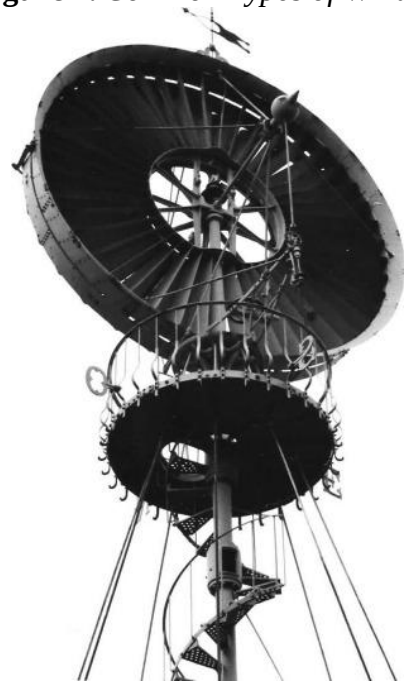

a) American farm HAWT (Bukala et al., 2015)

b) 3-bladed HAWT (Lee et al., 2016)

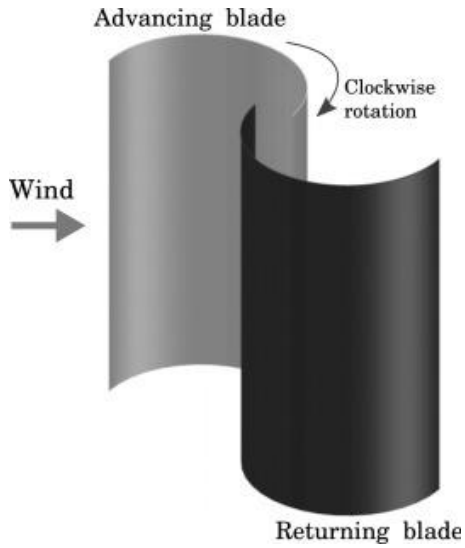

c) Savonius VAWT (Roy and Ducoin, 2016)

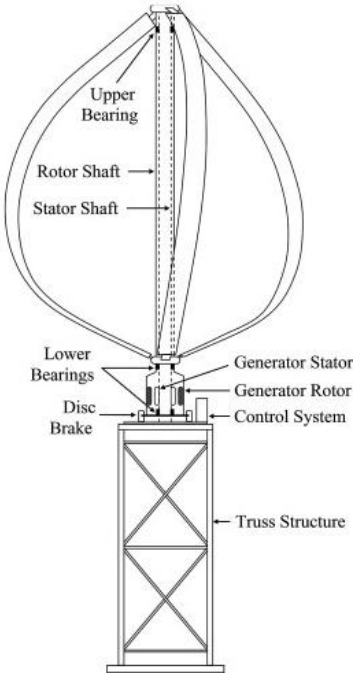

d) Darrieus VAWT (Tjiu et al., 2015)

Table 1 shows a comparison between HAWT and VAWT turbines. It shows that VAWT turbines are more practical than HAWT in terms of fabrication, cost, noise, and possibility to operate at low wind speed conditions whereas HAWT are better in terms of efficiency and reliability.

Table 1. *Characteristics of VAWT and HAWT Wind Turbines*

Type	VAWT	HAWT
Advantages	Easy to maintain	Good stability
	Low construction & maintenance costs	Self-starting
	No need for adjustment to wind direction	High reliability
	Low noise	High efficiency
	Operates at low wind speeds	
Disadvantages	Low efficiency	High maintenance costs
	Very low starting torque	Complex fabrication & installation
		High noise level

Figure **2** shows the operating range curves. It can be seen that the turbine type with the lowest operating tip speed ratio is the Savonius type turbine. Therefore, it is the most suitable candidate for producing a small scale wind turbine.

Figure 2. *Betz Limit for Several Types of Wind Turbines (Van Kuik, 2007)*

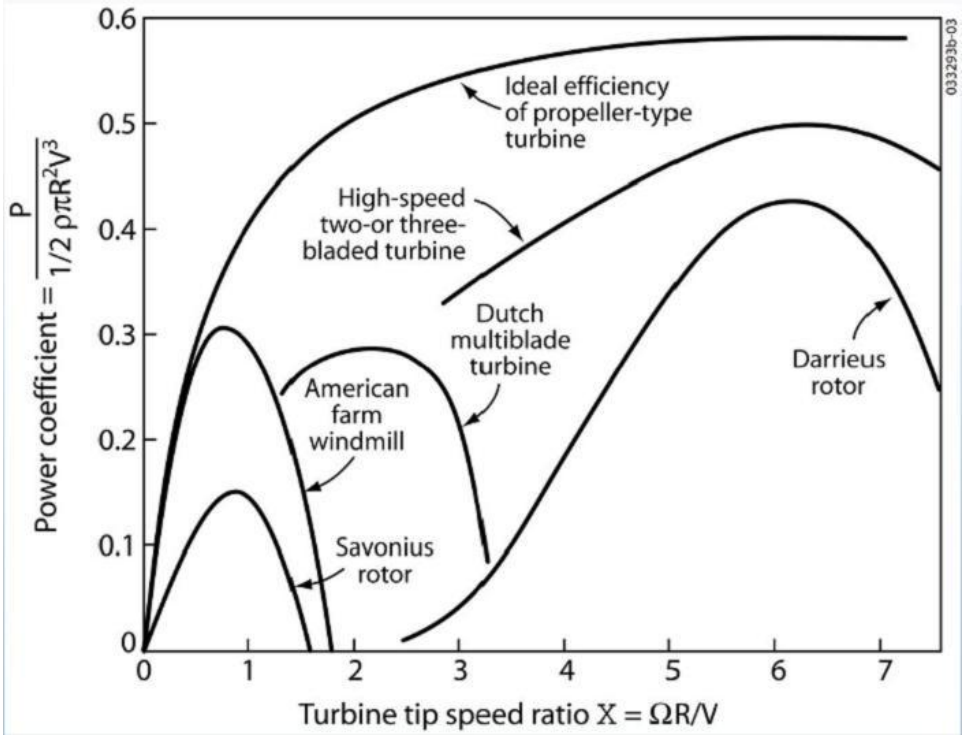

Aerodynamic Analysis

The design approach adopted in this paper consists of experimental testing in a wind tunnel on a small-scale model for different blade designs and airfoil shapes in order to choose the best configuration. But first, an analytical calculation was carried out in order to estimate some variables for different operating conditions. Three types of VAWT were tested: one type of Savonius turbine and two types of Darrieus turbine. NACA0021 and NACA2412 airfoil profiles were tested for the Darrieus type but the results were not encouraging in the case of low speeds. Therefore, The Savonius type was adopted to carry out further experiments since it works on drag and provides better results in the desired operating conditions. The rotational speed of the turbine was measured with the help of a tachometer at different wind velocities for 3-bladed and 5-bladed Savonius turbines. The results are presented in **Error! Reference source not found.**.

Figure 3. *Rotational Speed versus Wind Speed*

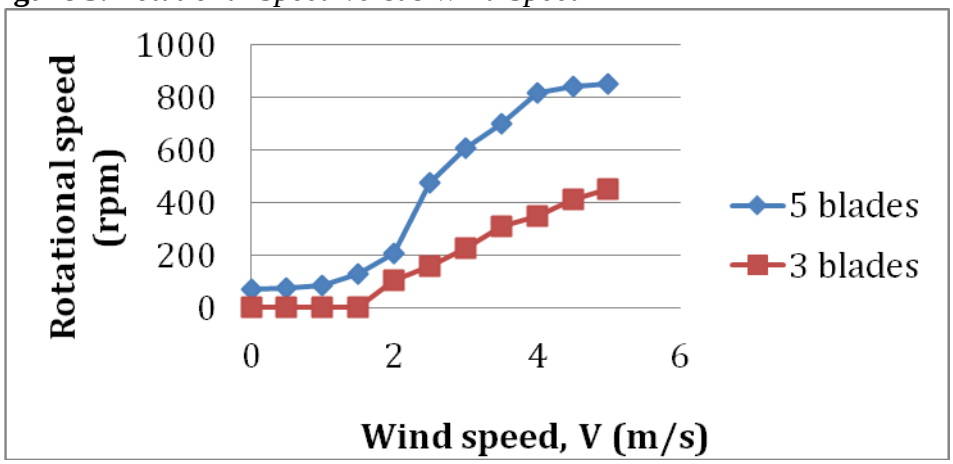

The power extracted from a single blade was analytically calculated for different blade radii, at several values of the tip speed ratio. The results are presented in

Figure **4**. The tip speed ratio λ is the ratio of the blade speed to the wind velocity, and it directly affects the performance of the turbine. Different types of wind turbines have different optimal tip speed ratio. Therefore, λ is a variable that depends on the geometry of the turbine and its components. In the obtained results, the maximum attained power corresponds to an optimal value of the tip speed ratio around 0.5 if a single blade is considered.

Figure 4. *Power Extracted from a Single Blade versus Blade Radius and Tip Speed Ratio*

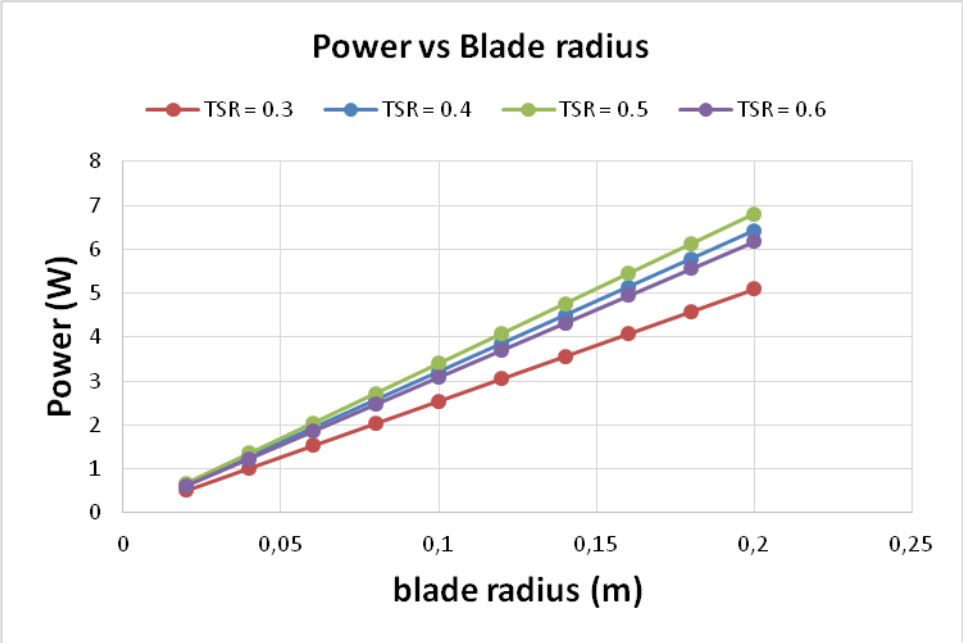

The previous result obtained for a single blade does not perfectly match with the result of a multi-blade turbine. Since the turbine is rotating, the blades will not be running at the same velocity with respect to the wind. In

Figure **5**, the relative velocity vector is shown for each blade of the turbine. It can be seen that some blades do not help the rotation of the turbine, but, contrarily, they constitute a load opposing to the rotation. However, the overall torque will result in the rotation of the turbine at a certain angular velocity.

Figure 5. *Relative Velocity Vector at Each Blade*

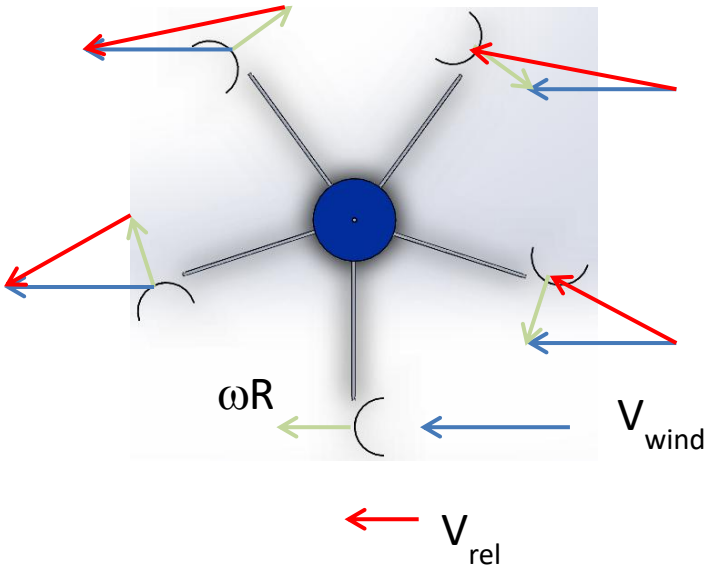

The optimal tip speed ratio for a 5-bladed Savonius turbine is around 1 (Van Kuik, 2007). The expected power extracted from the wind turbine is

plotted versus the wind speed in Figure 6. Two curves are plotted: one for the maximum case where the power coefficient equals the Betz limit of 59% and one for an expected power coefficient of 15%.

Figure 6. *Power vs Wind Speed for Different Power Coefficients*

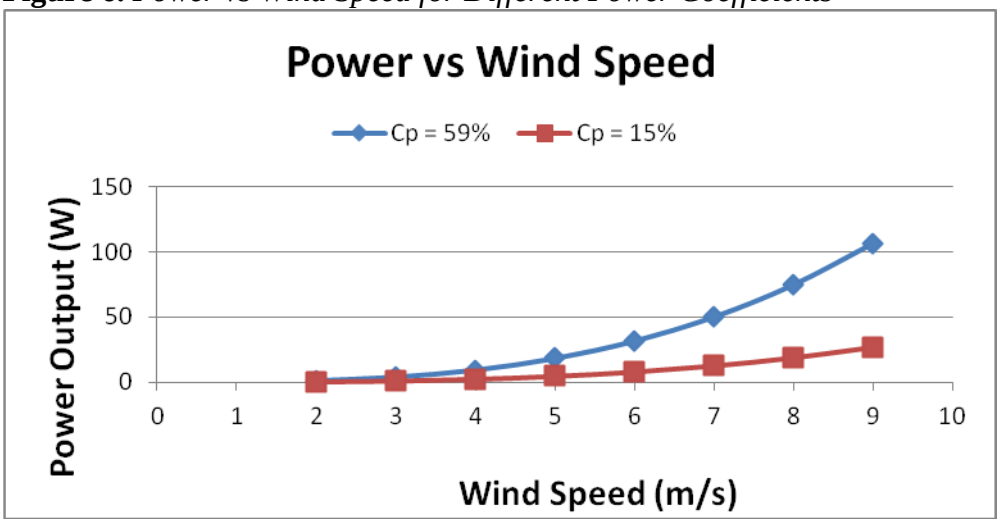

Structural Analysis

In order to properly size the different parts of the system, a finite element analysis using MSC PATRAN/NASTRAN was conducted.

Figure 7. *Geometry of the Wind Turbine for FE Analysis*

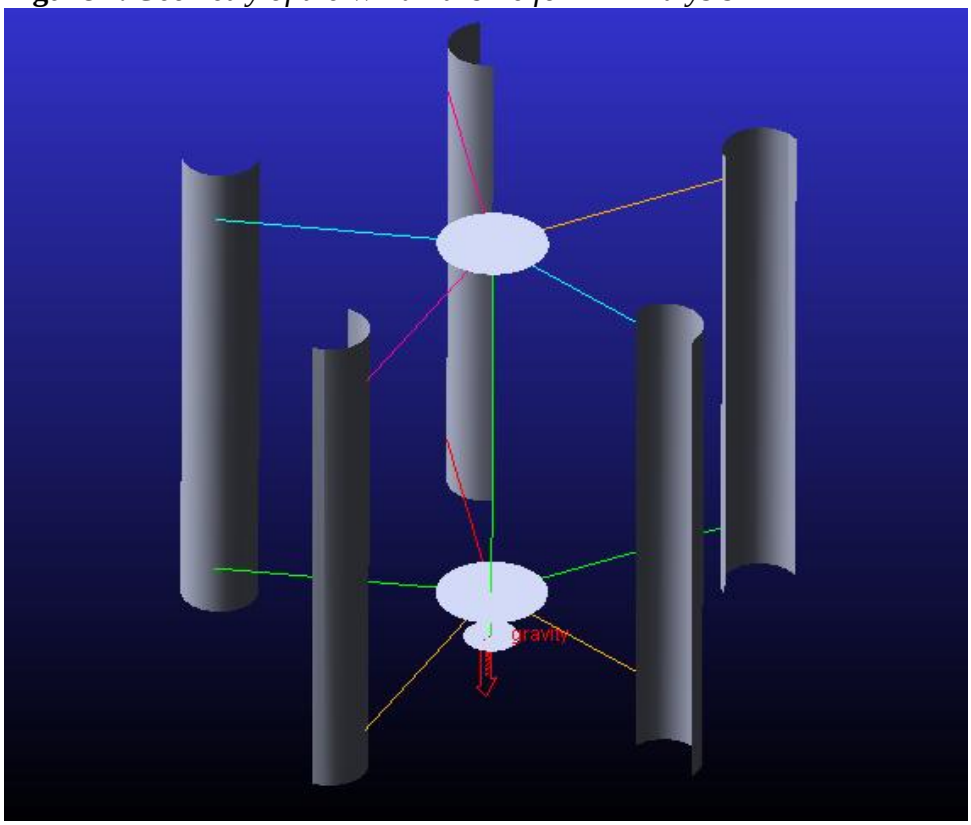

Shell elements (Quad4) were used for the disks and the blades, and 1D beam elements for the connecting rods and the shaft (

Figure **7**). The resulting model contains a total of 7854 elements with an average element size of 5 mm (

Figure **8**). All parts are made of an aluminum alloy except for the blades that are made of fiberglass.

Figure 8. *FEM of Wind Turbine*

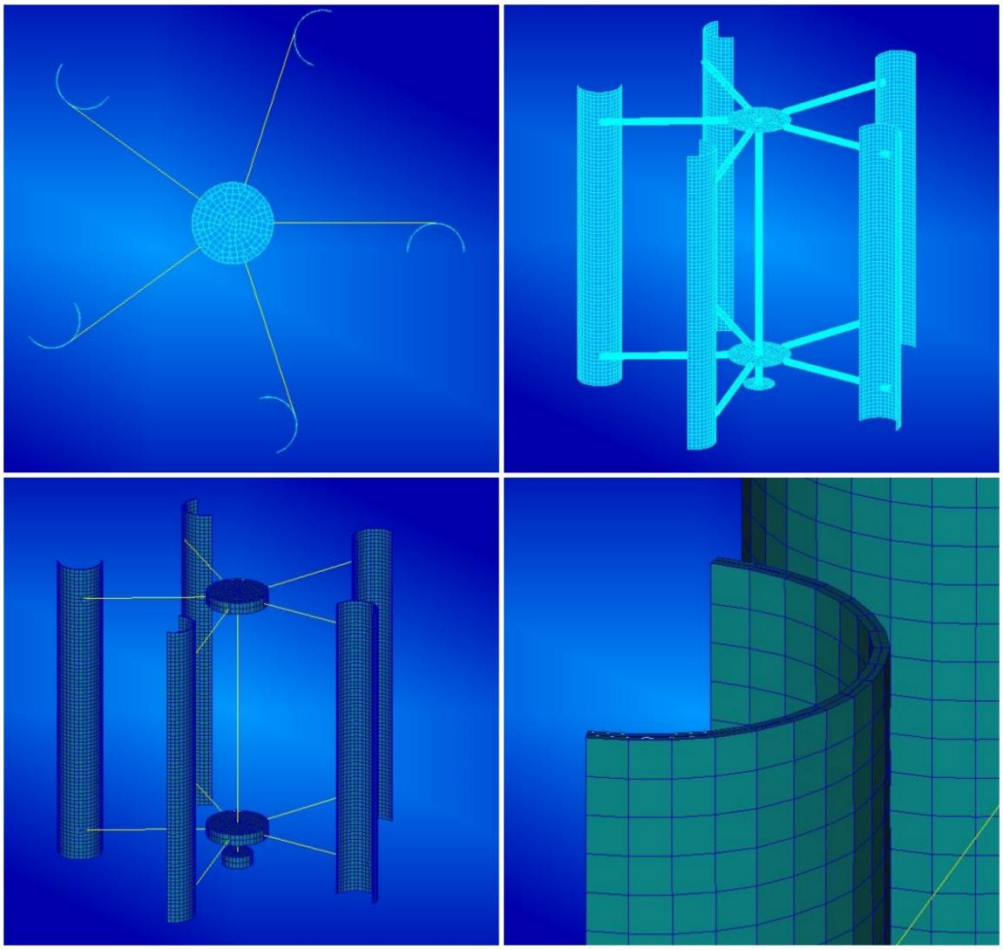

In order to assess the structural integrity of the system, two extreme load cases were considered. In the first case, a normal operation of the turbine is assumed in which the blades are rotating and centrifugal forces are transmitted into the connecting rods. In the second load case, the turbine is assumed to be blocked due a malfunctioning of the system, and the same uniform pressure is applied to all the blades simultaneously.

Load Case 1

This case consists of centrifugal forces (

Figure **9**) that are calculated by using the following formula:

$$F_{CF} = m_r \times R \times \omega^2$$

Where:

m_r : Mass of the blade in *kg*
R : Radius of the turbine in *m*
ω : Rotational speed in *rad/s*

Figure 9. *Centrifugal Force Placement*

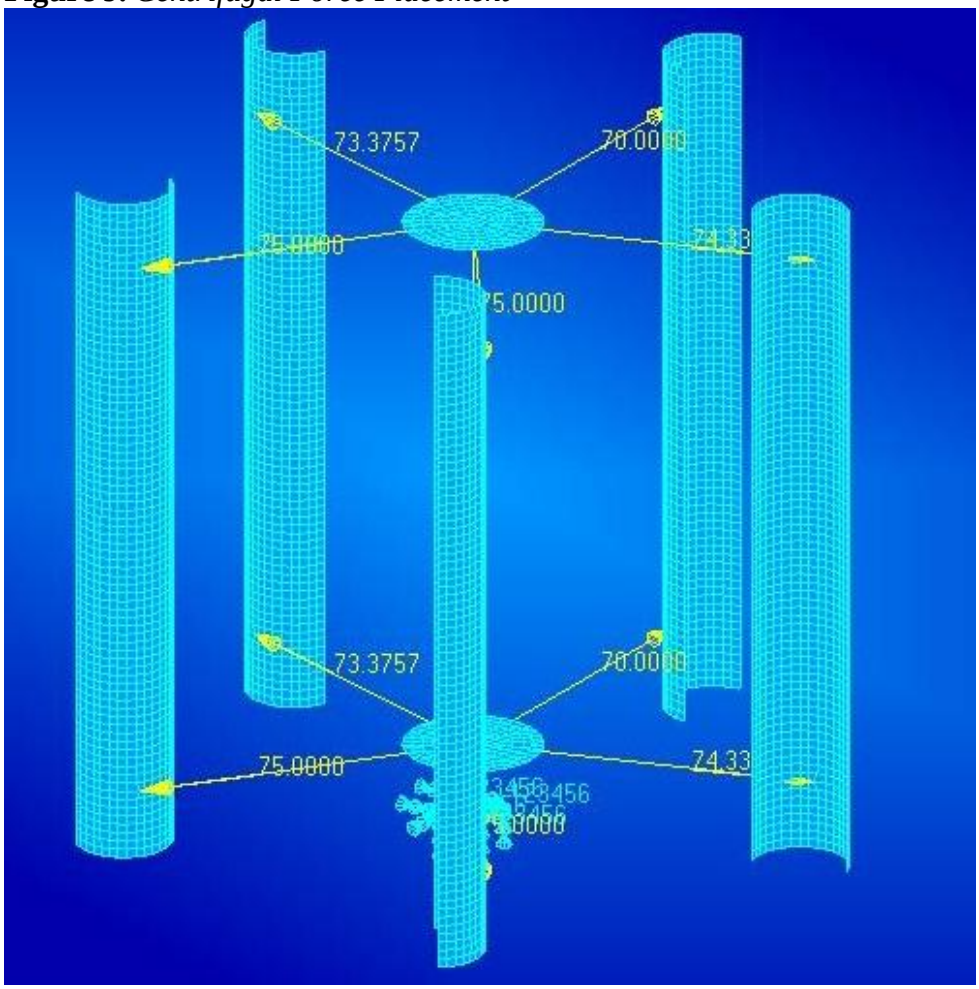

It can be seen from the results of the first case that the maximum stresses are 34 *MPa* for the Von Mises stress distribution for the shell elements (

Figure **11**) and 23.5 *MPa* for the combined stress distribution for the beam elements (

Figure **12**). Hence the resulting factors of safety are:

$$n_{Von-Misses} = 3.5$$

$$n_{Combined-Stress} = 5.4$$

Also a maximum deformation of 0.134 *cm* was recorded (

Figure **10**).

Figure 10. *Deformation Distribution for Load Case 1*

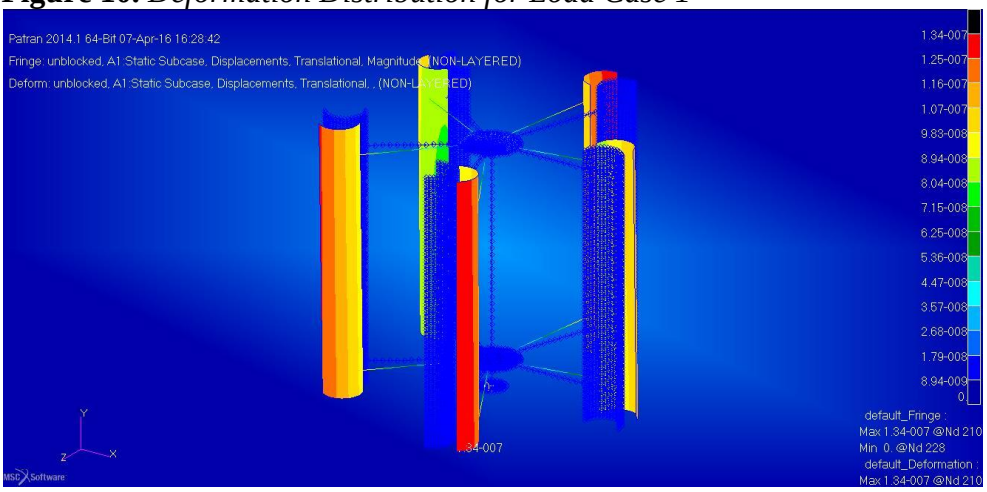

Figure 11. *Von Mises Stress Distribution for Load Case 1*

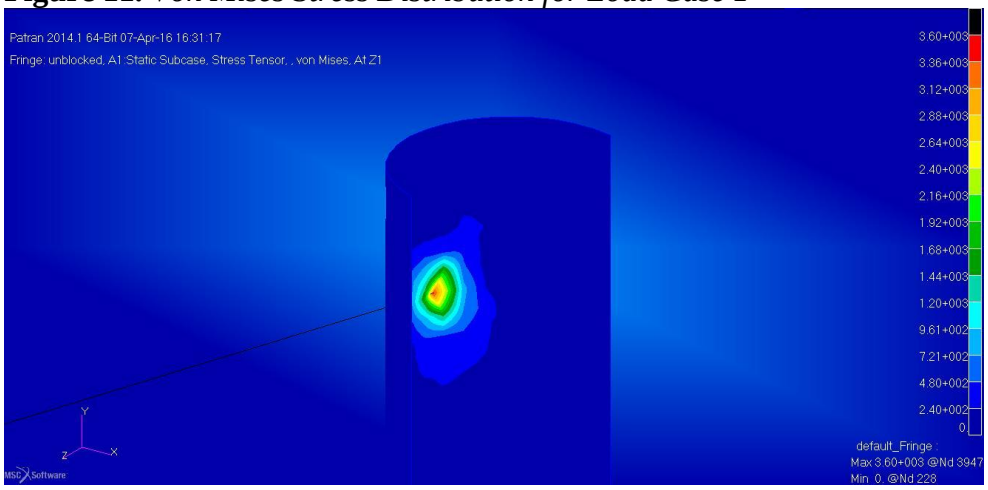

Figure 12. *Combined Stress Distribution for Load Case*

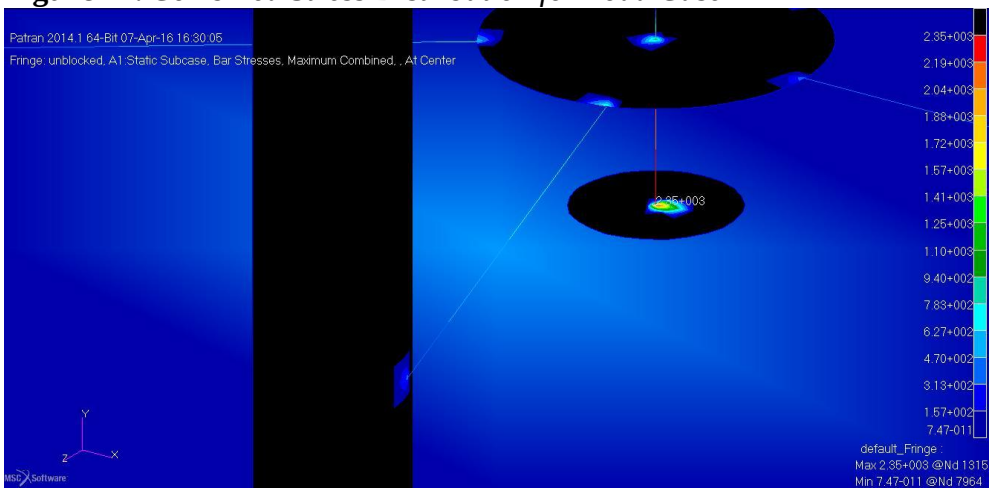

Load Case 2

This case consists of a uniformly distributed pressure along the blades of the turbine (

Figure **13**).

Figure 13. *Loads and BC's for Load Case 2*

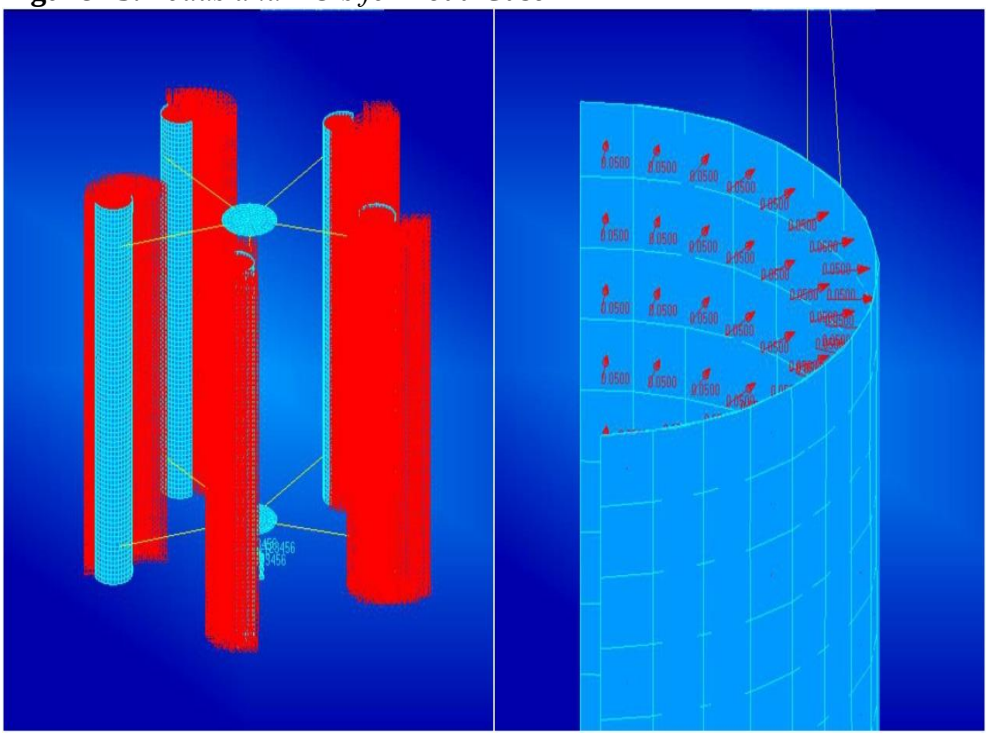

Results show a maximum Von Mises stress of 113 MPa (

Figure **15**) and a maximum combined stress 34 MPa (
Figure **16**) resulting in the following factors of safety:

$$n_{Von-Misses} = 1.1$$
$$n_{Combined-Stress} = 3.7$$

Also a maximum deformation of 1.15 *cm* was recorded (Figure 14).

Figure 14. *Deformation Results for Load Case 2*

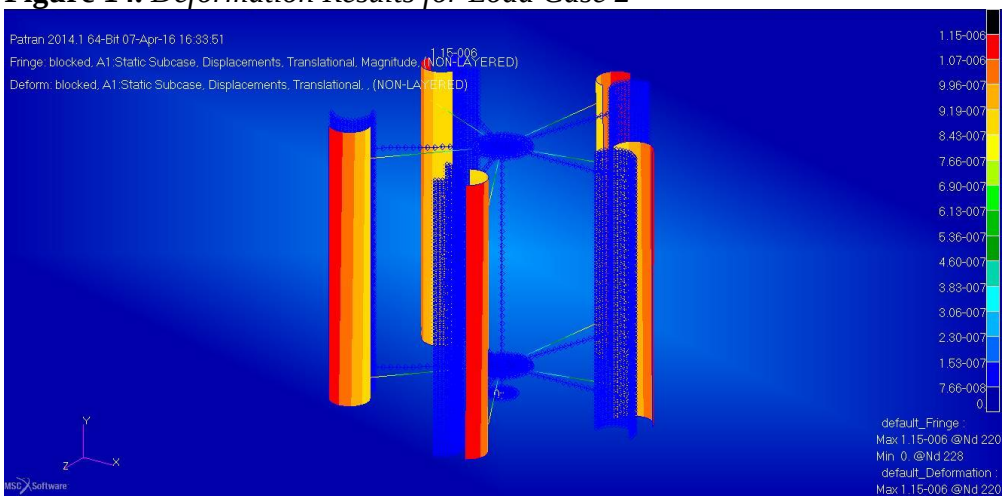

Figure 15. *Von Mises Stress Distribution for Load Case 2*

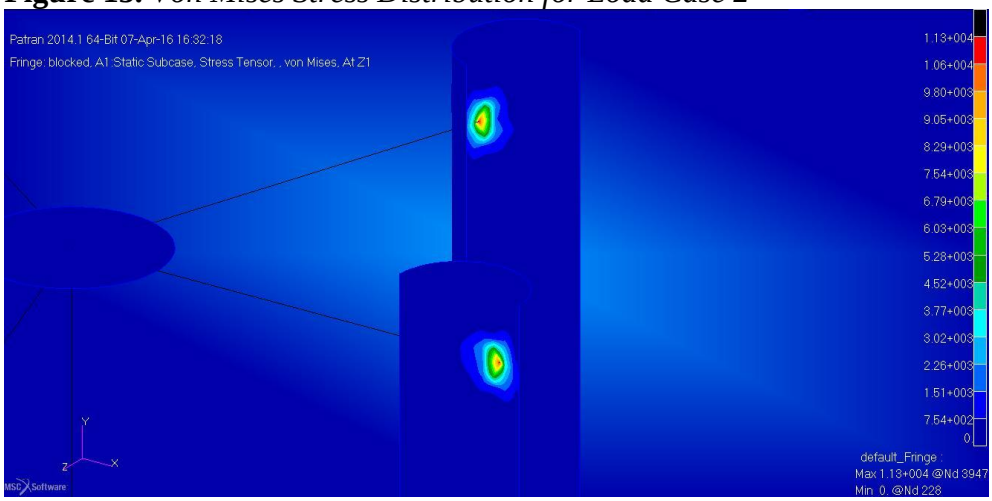

Figure 16. *Combined Stress Distribution for Load Case 2*

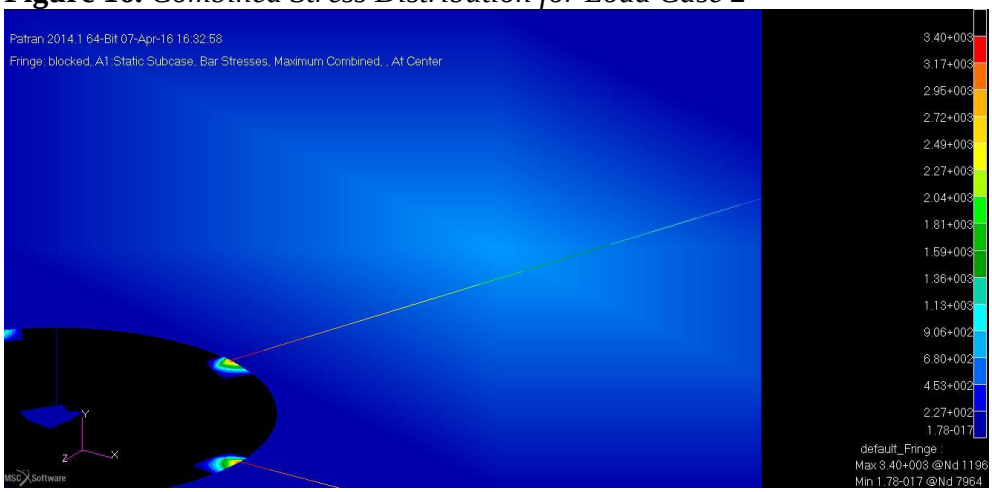

Even though the values for the second case are on the edge of what could be considered critical, the loading is extremely exaggerated since the assumption that the pressure on each blade is the same is impractical. Moreover the maximum stresses are due to a singularity at the connection of a 1D beam element with a 2D shell element. Consequently, the stresses will be lower in reality.

Multibody Dynamics

In order to assess the performance of the system, a multibody dynamics simulation using MSC ADAMS was performed.

MSC ADAMS was used in order to specify the characteristics of the generator that will be used to convert the mechanical input power which is related to torque and rotational speed into electrical output power which is related to the terminal voltage and the armature current. The value that will be sought after is the magnetic field inside the generator by fixing the other characteristics such as the type, number of poles and armature resistance according to the generator type that is most available.

In addition to the performance of the turbine, forces can be calculated at key positions such as connectors.

The turbine was first modelled on SolidWorks and then it was exported as a parasolid file which can be directly imported into MSC ADAMS (

Figure **17**).

Figure 17. *VAWT Model on MSC ADAMS*

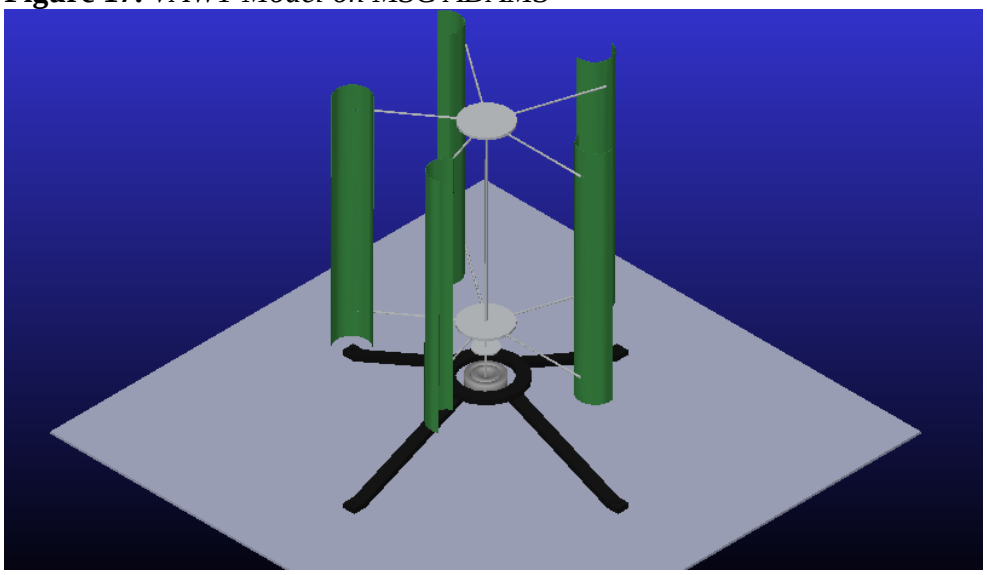

A series of machinery, joints and loads were then used to define the case of a rotating vertical axis that is held up by a bearing and that is locked with the central disks which is also locked with the handles and the blades. The handles and the blades are connected by a fixed joint, the base plate and the handles are also connected by a fixed joint. A bearing is fixed to the support and rotates freely with the central rod about the vertical axis. The support of the turbine is fixed to the ground body via four fixed joint connectors.

Due to the low rotational speed of the turbine, a system of pulleys (

Figure **18**) was added by using the inbuilt pulley systems in MSC ADAMS. At the end of the output shaft a motor was attached that had no source voltage (0 source voltage); hence it acted as a generator for the turbine, the motor was specified to operate according to direct current (DC). The motor can either be specified analytically, based on a torque-RPM curve or by an external program. In this simulation, an analytical motor was applied to the turbine and by trial and error the magnetic flux of the motor was modified in order to achieve the required output power. Given that the rotational speed of the turbine was around 30 *RPM*, a ratio of 25 was taken for the pulley to ensure that a rotational speed ranging from 600 to 800 *RPM* was achieved on the output shaft.

Figure 18. *System of Pulleys*

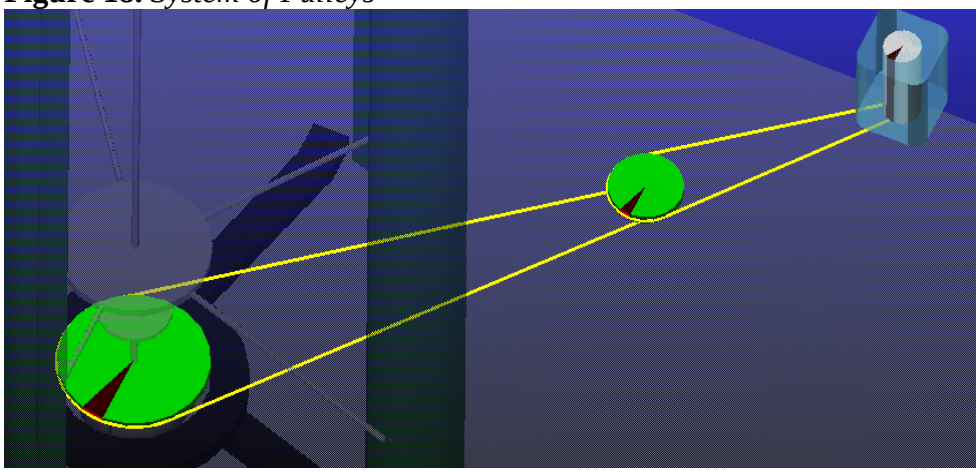

From the loads on the blades previously calculated, a torque of 566 N.mm corresponding to a wind speed of 8 m/s was computed and applied to the central rotating rod (
Figure **19**).

Figure 19. *Torque Application on Central Rod*

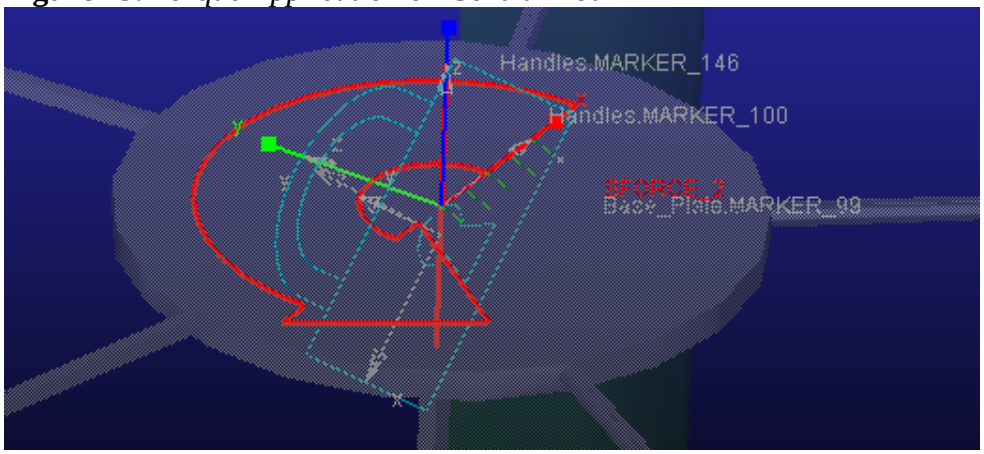

The following procedure was used in order to get the characteristics of the generator:

1. Set the time of the simulation to 5 seconds with 0.1 seconds increments.
2. Set the Torque at the Turbine to the required value.
3. Adjust the Magnetic Flux of the Generator.
4. Measure the Power and Rotational Speed of the Generator.
5. Compare results with previous tests to increase or decrease the value of the Magnetic Flux.
6. Repeat until required parameters of the Generator are achieved.

Finally the obtained generator characteristics were:

- DC Generator with 4 Poles, Shunt, 2 paths.
- Number of Conductors = 100.
- Flux per Pole: $\phi = 135mWb$

The variation of output power, rotational speed and torque at the generator is shown in

Figure **20**, Figure 21, and Figure 22 respectively.

Figure 20. *Power Variation*

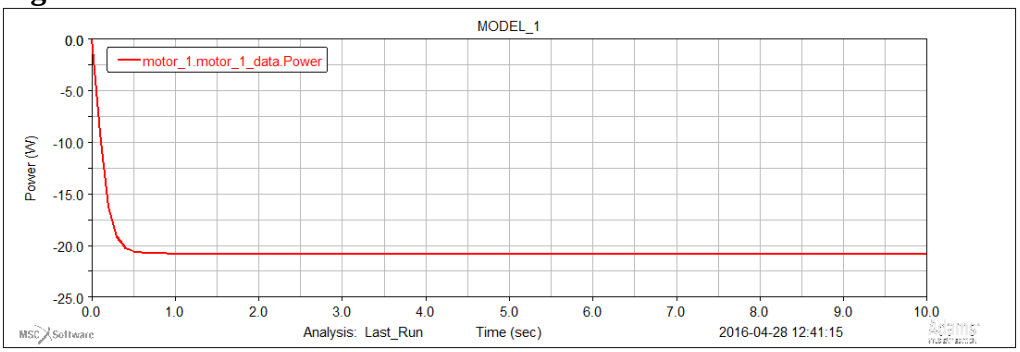

Figure 21. *RPM Variation*

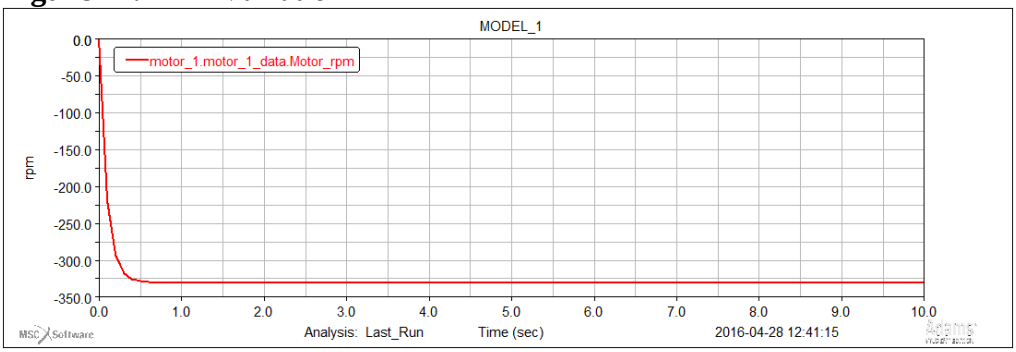

Figure 22. *Torque Variation*

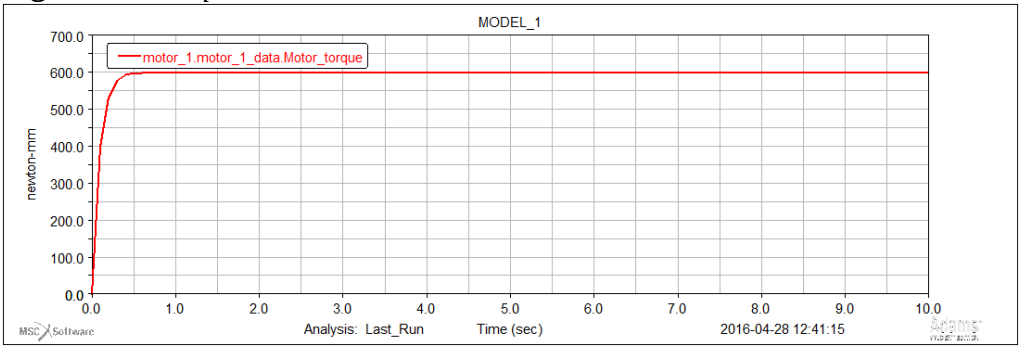

Prototype Manufacturing

All of the turbines' structural parts are made of aluminum except the blades which are made out of fiberglass. This results in a reduced total weight and a concentration of weight on the axis of rotation which reduces the effects of out of balance vibrations at high speeds. The fixed support is

manufactured of steel adding structural rigidity and stability to the system. The blades were 1 *m* long, an inner diameter of 11 *cm* and a thickness of 1 *mm* (Figure 23). For ease of fabrication, the blades were moulded by using a semi cylindrical sewage pipe.

Figure 23. *Isometric View of the Blade (Units in Meters)*

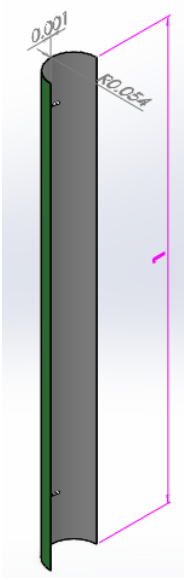

To fabricate the blades from fibre glass material (type CSM), a duct is cut into 2 symmetrical parts. The 2 parts constitute the mould for 2 blades. A non-perforated release film is used to prevent the bonding of the fibre glass on the mould. The process of fabrication is a hand layup. Each blade consists of 2 layers of glass fibres. A polyester resin is used with a ratio of 50% of the total product. A hardener is added to the resin with a ratio of 2%. The curing time is about 24 hours. After removing the blades from the mould, the edges are cut with the proper dimensions. Finally, these components are assembled all together and connected to a well welded steel support, via 2 bearings, to form the final product (

Figure **24**).

Figure 24. *Final Assembly of the Turbine*

Experimental Validation

Experimental tests were carried out in a PLINT wind tunnel of a cross sectional area 30×30 cm^2 for various wind speeds up to 17 m/s. The wind velocity was measured with the help of a Pitot tube. Geometric and dynamic similarities were satisfied between model and prototype.

In order to measure the torque produced by the turbine, a breaking system was rearranged in such a way that it can be connected to a pulley that has a bucket at the other end in which a certain weight must be added in order to stop the rotation of the turbine by engaging the brake pads.

The tip speed ratio was measured for several wind speeds (

Figure **25**). Low values ranging between 0.3 and 0.55 were obtained. The power coefficient was also measured and is presented in Figure 26. A power coefficient around 5% was obtained because of low tip speed ratio. At higher velocities, turbulence and vibrations occurred and disturbed the normal operation of the turbine.

Figure 25. *Tip Speed Ratio vs Wind Speed*

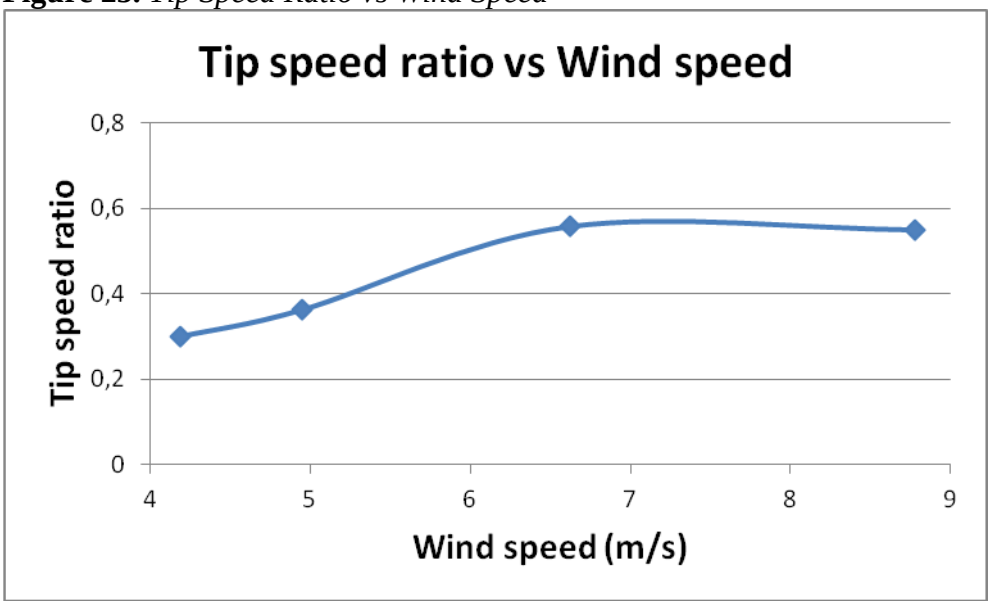

Figure 26. *Power Coefficient vs Tip Speed Ratio*

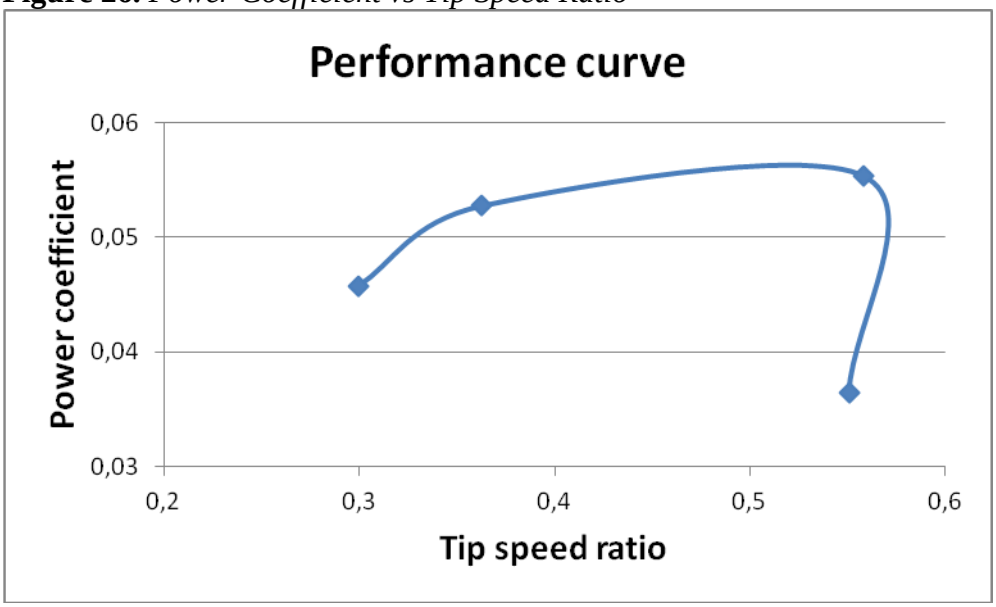

A comparison between the expected and actual power outputs was carried out and is shown in

Figure **27**. The expected power and actual power output are very similar especially at low speeds. At high wind speeds, the actual power falls short of the expected power; this is due to the fact that at high wind speeds the wind turbine started to vibrate which caused a loss in power and the braking system to slip.

Figure 27. *Comparison between Expected and Actual Power*

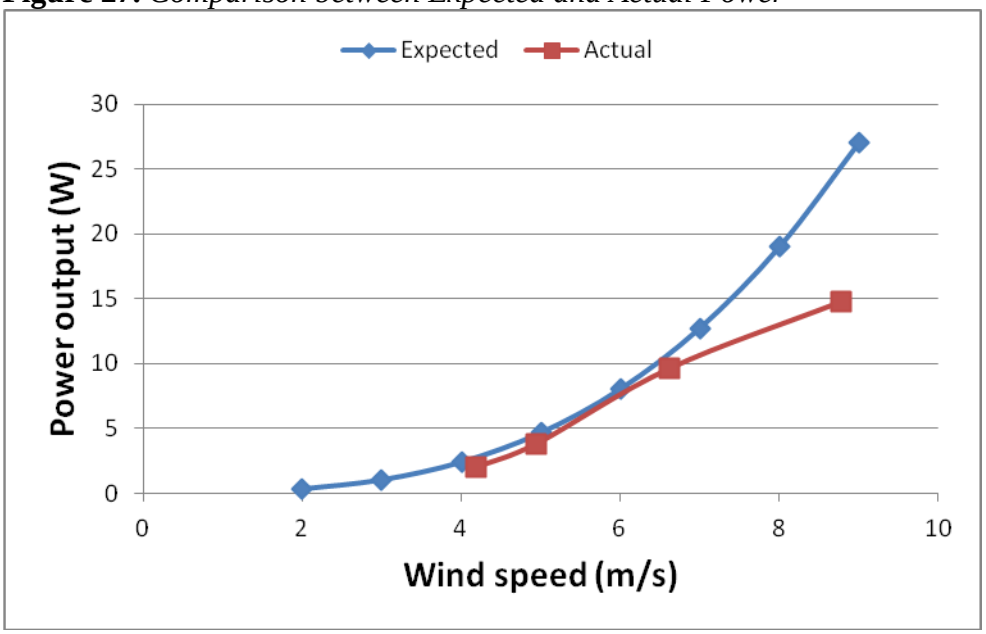

In

Figure **28**, the actual curve of the rotational speed is being fitted to 2 analytical curves. It was observed that for low wind speeds, the actual curve follows the behaviour of the expected one at a tip speed ratio of 0.3. However, for higher speeds, the actual curve gets closer to the expected one at a tip speed ratio around 0.5.

Figure 28. *Comparison between Calculated and Actual Rotational Speed at Different Tip Speed Ratios*

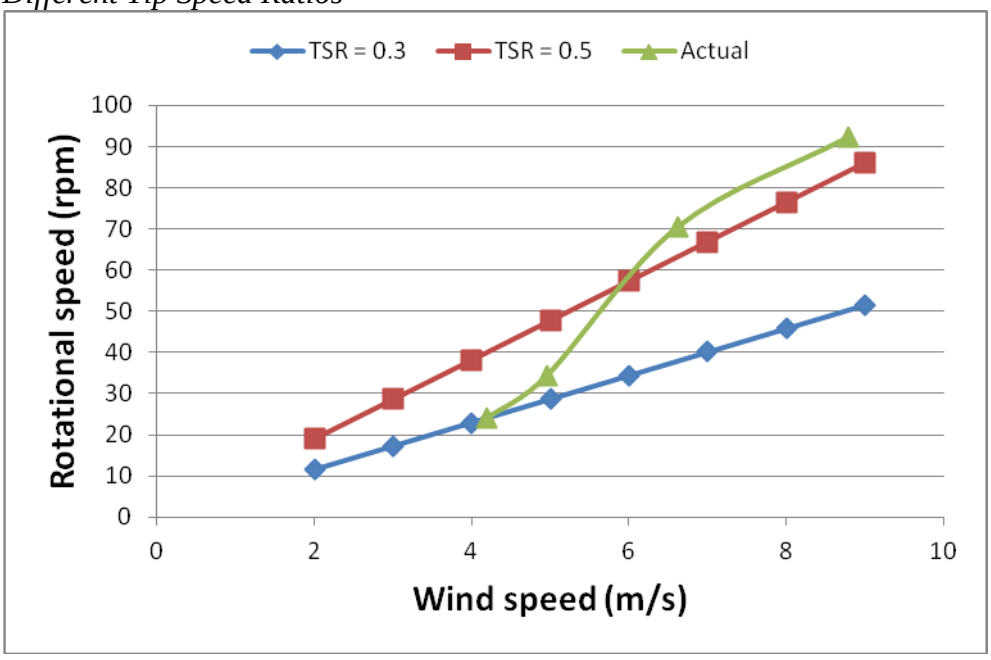

The following conclusions were deducted from experimental measurements:

1. Increasing the wind speed increases the rotational speed, torque and power output of the turbine.
2. Many curves are needed to expect the behaviour of the turbine, providing a certain range for its operation.
3. The maximum power output was around 15 Watts.

The low power obtained from experimental results is due to several reasons: first, the size of the turbine was limited in order to fit with wind tunnel tests; second, the inaccuracies in torque measurement using the breaking system. However, the global behavior of the turbine was found to be in accordance with expectations.

In order to supply a household with a similar turbine, the required output power must be calculated from the electric consumption of the appliances. Then, based on the similarity in terms of performance coefficient, the size of a desired actual turbine could be determined. For example, for a 1-kW power, considering an average performance coefficient of 0.055, a turbine having a length of 9.6 m and a radius of 3.37 m will be required to generate this amount of power.

Conclusions

It can clearly be seen that the Savonius type turbine is not efficient in terms of output power; however, the advantage of such a type of turbine lies in the operating range because this VAWT can operate under low wind speeds.

MSC ADAMS recorded a power of 22 Watts with an ideal generator that had no armature resistance at a wind speed of 8 *m/s*. The actual results at a wind speed of 8.5 *m/s* recorded an output power of 14.5 Watts. The results; although different, are comparable and it can be seen that a mechanical loss of 7.5 Watts generated by the friction and the vibrations of the turbine if the power recorded by MSC ADAMS is taken as a reference.

In conclusion, the manufacturing and testing of a Savonius type VAWT was done, the selection of the Savonius type VAWT is due to the fact that it can operate under low wind speeds. In addition, a dynamic simulation using MSC ADAMS to get the configurations of the generator and the forces on the connecting joints and a stress analysis using MSC PATRAN were conducted in order to estimate the performance and to verify the structural integrity of the turbine. Then the turbine was assembled and tested by using a wind tunnel in order to preserve the consistency of the testing conditions and to avoid the fluctuating natural wind, a series of measurement apparatus were used in order to get the wind speed just before the turbine and the corresponding torque and rotational speed of the turbine. The test results were in accordance with the theoretical results. The proposed sizing methodology will enable sizing wind turbines of higher power outputs. In addition, wind turbines with different radii of blades may be tested in order to improve the coefficient of performance.

References

Balduzzi F., Bianchini A., Maleci R., Ferrara G., Ferrari L., (2016). *"Critical issues in the CFD simulation of Darrieus wind turbines"*, Renewable Energy, Volume 85, Pages 419-435, ISSN 0960-1481.

Bukala J., Damaziak K., Karimi H.R., Kroszczynski K., Krzeszowiec M., Malachowski J., (2015). *"Modern small wind turbine design solutions comparison in terms of estimated cost to energy output ratio"*, Renewable Energy, Volume 83, Pages 1166-1173, ISSN 0960-1481.

Can K., Feng Z., and Xuejun M.. (2010). "*Comparison study of a vertical-axis spiral rotor and a conventional Savonius rotor",* Asia-Pacific Power and Energy Engineering Conference. IEEE.

Darrieus G.J.M. (1931). *"Turbine Having its rotating shaft transverse to the flow of the current"*. US Patent No. 1835081.

Eriksson S., Bernhoff H., and Leijon M., (2008). "*Evaluation of different turbine concepts for wind power"* Renewable and Sustainable Energy Reviews 12.5: 1419-1434.

Kaldellis J., and Zafirakis D., (2011). *"The wind energy (r) evolution: A short review of a long history",* Renewable Energy 36.7: 1887-1901.

Lee M.H., Shiah Y.C., Bai C.J., (2016). *"Experiments and numerical simulations of the rotor-blade performance for a small-scale horizontal axis wind turbine"*, Journal of Wind Engineering and Industrial Aerodynamics, Volume 149, Pages 17-29, ISSN 0167-6105.

Li Q., Murata J., Endo M., Maeda T., Kamada Y., (2016). *"Experimental and numerical investigation of the effect of turbulent inflow on a Horizontal Axis Wind Turbine (part II: Wake characteristics)"*, Energy, Volume 113, Pages 1304-1315, ISSN 0360-5442.

Righter, R., (1996). *"Wind energy in America: A history",* University of Oklahoma Press.

Roy S. and Saha U.K. (2013). *"Review on the numerical investigations into the design and development of Savonius wind rotors"*. Renew Sustain Energy Rev, 24, pp. 73–83.

Roy S. and Ducoin A., (2016). *"Unsteady analysis on the instantaneous forces and moment arms acting on a novel Savonius-style wind turbine"*. Energy Conversion and Management, Volume 121, Pages 281-296, ISSN 0196-8904.

Tjiu W., Marnoto T., Mat S., Ruslan M.H., Sopian K., (2015). *"Darrieus vertical axis wind turbine for power generation I: Assessment of Darrieus VAWT configurations"*, Renewable Energy, Volume 75, Pages 50-67, ISSN 0960-1481.

Van Kuik, G, (2007). "*The Lanchester–Betz–Joukowsky limit",* Wind Energy 10.3: 289-291.

Wilson M., (1969). *"Energy",* Life Science Library.

Yannopoulos, S.I.; Lyberatos, G.; Theodossiou, N.; Li, W.; Valipour, M.; Tamburrino, A.; Angelakis, A.N., (2015). *"Evolution of Water Lifting Devices* (*Pumps*) *over the Centuries Worldwide",* Water 7, 5031-5060.